

NACA  
RM-L9B10



# RESEARCH MEMORANDUM

AN ANALYSIS OF AVAILABLE DATA ON EFFECTS OF WING-  
FUSELAGE-TAIL AND WING-NACELLE INTERFERENCE  
ON THE DISTRIBUTION OF THE AIR LOAD  
AMONG COMPONENTS OF AIRPLANES

By

Bertram C. Wollner

Langley Aeronautical Laboratory  
Langley Air Force Base, Va.

#### CLASSIFIED DOCUMENT

This document contains classified information affecting the National Defense of the United States within the meaning of the Espionage Act, USC 50:31 and 32. Its transmission or the revelation of its contents in any manner to an unauthorized person is prohibited by law. Information so classified may be imparted only to persons in the military and naval services of the United States, appropriate civilian officers and employees of the Federal Government who have a legitimate interest therein, and to United States citizens of known loyalty and discretion who of necessity must be informed thereof.

NATIONAL ADVISORY COMMITTEE  
FOR AERONAUTICS

WASHINGTON

April 11, 1949



~~UNCLASSIFIED~~

## NATIONAL ADVISORY COMMITTEE FOR AERONAUTICS

## RESEARCH MEMORANDUM

AN ANALYSIS OF AVAILABLE DATA ON EFFECTS OF WING-  
FUSELAGE-TAIL AND WING-NACELLE INTERFERENCE  
ON THE DISTRIBUTION OF THE AIR LOAD  
AMONG COMPONENTS OF AIRPLANES

By Bertram C. Wollner

## SUMMARY

Available information on the effects of wing-fuselage-tail and wing-nacelle interference on the distribution of the air load among components of airplanes is analyzed. The effects of wing and nacelle incidence, horizontal and vertical position of wing and nacelle, fuselage shape, wing section and filleting are considered.

Where sufficient data were unavailable to determine the distribution of the air load, the change in lift caused by interference between wing and fuselage was found. This increment is affected to the greatest extent by vertical wing position.

## INTRODUCTION

At the design points on the V-n diagram where the magnitude of the over-all load is given by specification, it is commonly assumed that the wing either carries all the load or the fuselage carries the portion that would normally be carried by the intercepted wing area. These assumptions result in conservative designs for the wing if the loads carried by the fuselage and tail act in the same direction as that on the wing and in an unconservative design if they act in an opposite direction.

Along experimental lines there are very little data in the literature that can be used to determine the division of loads among the airplane components. So far as is known, the only tests in which directly useable data on the division of load are given are the flight tests described in references 1 and 2. Some indirect tests have been made, however, which apply to the general problem of the division of load. These are the tests performed in connection with the wing-fuselage interference program previously reported in references 3 and 4.

Classification Changed to	<b>UNCLASSIFIED</b>
Authority	<i>Actin Sec. of Defense Bulletin</i>
Date	<i>June 14 1954</i>
By	<i>al. C. Wollner</i>

/

~~UNCLASSIFIED~~

Along theoretical lines there are several methods that may be used to find the distribution of the air load among airplane components. References 5 to 7 are typical of these mathematical methods which are limited in use to special simplified cases.

The purpose of the present paper is to summarize the available data on the effects of wing-fuselage-tail and wing-nacelle interference on the distribution of the air load among aircraft components. The effects of wing and nacelle incidence, horizontal and vertical position of wing and nacelle, fuselage shape, wing section and filleting, are considered. Some discussion is also given of the effects of center-of-gravity position.

### SYMBOLS

In the analysis of the data, the following symbols have been adopted:

$C_L$	lift coefficient (Lift/ $qS$ )
$q$	dynamic pressure, pounds per square foot
$S$	gross wing area, square feet
$M$	Mach number
$\alpha$	angle of attack of wing chord line at model center line, degrees
$x$	longitudinal displacement of airfoil quarter-chord axis from fuselage quarter-chord point in terms of wing mean chord
$x_N$	longitudinal displacement of nacelle quarter-chord point from wing quarter-chord axis in terms of wing mean chord
$z$	vertical displacement of airfoil quarter-chord axis from fuselage axis in terms of wing mean chord
$z_N$	vertical displacement of nacelle axis from airfoil quarter-chord axis in terms of wing mean chord
$i$	wing angle of incidence with respect to fuselage axis, degrees
$i_N$	angle of incidence of nacelle axis with respect to wing chord line at nacelle position, degrees

## Subscripts:

A	airplane
W	wing
F	fuselage
WF	wing-fuselage combination
T	tail
N	nacelle
WN	wing-nacelle combination
a	indicates that component was tested alone and not in the presence of other components

In order that results may be compared on an equal basis all coefficients, regardless of the model configuration, are based on the gross wing area, that is, with the wing projected through the body.

## METHODS AND RESULTS

The division of load between such major items as the wing, fuselage, and tail can be determined by measurements of the load on each item by means of strain gages or pressure distributions with all the bodies in combination. In this paper these are termed direct measurements. Since direct data are limited to a very few sources additional information has been obtained from other measurements in which the forces on the individual components and on the combination were measured. Since in such tests the force on each component is not measured in the presence of the other components, the exact division of load cannot be found directly. In this paper such measurements are referred to as indirect measurements.

## Direct Data

Figures 1 and 2 present the available data which are directly applicable to show the division of the air load. The data shown in these figures are derived from flight measurements of wing and tail loads by means of strain gages located near the wing-fuselage and fuselage-tail junctures. The over-all loads on the airplane were determined from accelerometer measurements and from a knowledge of the airplane weight.

Figure 1 shows  $C_L \sqrt{1 - M^2}$  due to wing, tail, and fuselage of the X-1 airplane (previously designated XS-1) plotted against  $C_{L_A} \sqrt{1 - M^2}$ .

The curves were taken directly from reference 1. The data shown in the figure cover a Mach number range from 0.27 to 0.80. Figure 2 shows  $C_L$  due to wing, fuselage, and tail for the test airplane of reference 2 plotted against the airplane lift coefficient. The curves of figure 2 are based on data obtained during the tests reported in reference 2; these data cover Mach numbers from 0.32 to 0.74.

The factor  $\sqrt{1 - M^2}$  in figure 1 in both the ordinate and abscissa appears in the original figure in reference 1. This factor was not used in the preparation of figure 2.

Table I presents a comparison of the slopes of the experimental curves of figures 1 and 2 with theoretical values. In computing the theoretical slopes the assumption that fuselage lift in a wing-fuselage combination is proportional to the wing area blanketed by the body (or more properly in the present cases, wing area between strain-gage stations) is used. The experimental data of the figures were reduced to the status of a wing-fuselage configuration by adding the tail lift to that of the wing. The theoretical slopes were determined by using both strip and lifting-line theory.

#### Indirect Data

Figures 3 to 10 present data which, although not directly applicable to the problem of the division of air load, may be used to obtain trends. The data in these figures were obtained from material available in references 3 and 4. In these reports the forces on the wing and fuselage were first measured independently and then the total force on the combination was found. The tests were made at low speed and at a Reynolds number of 3,100,000.

In analyzing these data several methods of presentation were considered. As it is impossible to determine the distribution of the load from data of this type, the change in lift caused by interference between wing and fuselage is found. It is assumed that this incremental lift coefficient acts on the wing in line with the common design assumption that the wing carries all the load.

References 3 and 4 are concerned with the "lift and interference" of the fuselage  $\Delta C_{L_F}$ , which is the difference between the lift coefficient of the wing-fuselage combination and that of the wing alone at a given angle of attack.

Hence,

$$\Delta C_{L_F} = C_{L_{WF}} - C_{L_{W_a}} \quad (1)$$

By definition

$$C_{L_{WF}} = C_{L_{W_a}} + C_{L_{F_a}} + \Delta C_L \quad (2)$$

where  $\Delta C_L$  is the increment in lift due to the interaction between the two components.

Consequently  $\Delta C_L$  is

$$\Delta C_L = \Delta C_{L_F} - C_{L_{F_a}} \quad (3)$$

and the assumption is made that

$$\Delta C_L = \Delta C_{L_W} \quad (4)$$

The vertical and horizontal wing positions with respect to the fuselage considered are shown in figure 3.

The variation of the incremental lift coefficient  $\Delta C_{L_W}$  with model lift coefficient at several wing angles of incidence over a wide range of vertical and horizontal wing positions is shown in figure 4 for a model consisting of a rectangular wing with an NACA 0012 airfoil and a round fuselage. Figure 5 shows the variation of  $\Delta C_{L_W}$  with  $C_{L_{WF}}$  at several wing angles of incidence and wing positions above and below the fuselage for a model made up of a round fuselage and a tapered wing with NACA 0018-09 sections. The effect of varying the vertical position of the wing for this model with and without tapered fillets is shown in figure 6. Varying angle of incidence at several vertical wing positions for a round fuselage in combination with a rectangular wing with NACA 4412 section is considered in figure 7. Corresponding tests on models with rectangular fuselages and wings with NACA 0012, 0018-09, and 4412 sections are given in figures 8, 9, and 10, respectively.

The datum or reference condition for figures 4 to 10 is the combination in each case with the wing one-quarter root chord point coincident with the fuselage one-quarter chord point ( $x = 0, z = 0$ ) and with the wing at zero angle of incidence ( $i_w = 0$ ). Unfortunately in order to use the results presented in these figures it is necessary to have a breakdown of the air load such as is given in figures 1 and 2 for the datum condition. The increment in lift measured from the reference condition of the given curves is then added to the corresponding value shown on the breakdown curve.

Figure 11 shows the various positions of the nacelle with respect to the wing considered in figures 12 to 14. These figures present indirect data that apply to the effects of wing-nacelle interference on the component loads. The data used were first presented in reference 8. The incremental lift coefficient as defined here is

$$\Delta C_{L_N} = C_{L_{WN}} - C_{L_{W_a}} \quad (5)$$

Insufficient data were available to isolate the lift due to wing-nacelle interference. Figures 11 to 14 consider the effects upon the incremental nacelle lift of varying the longitudinal and vertical position of the nacelle on the wing and the nacelle angle of incidence with respect to the wing independently of each other. The model consisted of a modified NACA fuselage form 111 with a fineness ratio of 6.0 in combination with a modified NACA 65-210 airfoil.

## DISCUSSION

### Lift on Components

The comparisons shown in table I indicate that the assumption that fuselage lift is proportional to the area of wing blanketed by the body is valid over the Mach number range covered by the flights for the two airplanes for which data are available. The discrepancies between flight and theoretical results may be due in part to the distribution of the tail lift between the other two components; the assumption that tail lift is entirely carried by the wing outboard of the strain-gage stations not being wholly correct.

The analysis of the data of figures 1 and 2 indicate little apparent variation of the division of the air load among the components of the airplane with Mach number within the range of the available flight tests.

The measurements of wing and tail lift coefficients for the X-1 airplane are accurate within  $\pm 0.025$ . The accuracy of the measurements of wing and tail lift coefficients of the test airplane of reference 2 was estimated to be within  $\pm 0.02$  and  $\pm 0.005$ , respectively. The factor  $C_{L_A}$  was estimated to have a maximum error of about  $\pm 0.04$  at the highest lift coefficients.

The effect of changing airplane center-of-gravity position on the distribution of the air load was found to be negligible for the test airplanes of figures 1 and 2. In the cases of larger airplanes, it is conceivable that movement of the airplane center of gravity may affect the component loads more noticeably. In general, a forward center-of-gravity movement will tend to decrease the tail lift, negative tail loads becoming more negative, while the wing lift will experience a corresponding increase.

#### Wing-Fuselage Interference

The results of the tests summarized in figure 4 show the incremental lift coefficient (assumed to act on the wing) to vary regularly with model lift coefficient and wing incidence except at vertical wing positions near the tangential where the variation becomes quite irregular.

At wing positions from  $z = 0$  to  $z = 0.26$  there is seen to be very little variation of  $\Delta C_{L_W}$  with the lift coefficient of the combination.

Increasing wing incidence tends to decrease the incremental lift coefficient, while the variation of  $\Delta C_{L_W}$  with the wing vertical position is negligible.

As the wing approaches the tangential position between  $z = 0.26$  and  $z = 0.40$  marked changes occur in the incremental lift coefficient. Its variation with the model lift becomes irregular, and the coefficient itself may attain unusually high values.

At wing positions above the fuselage from  $z = 0.40$  to  $z = 1.00$  the variation of  $\Delta C_{L_W}$  with  $C_{L_W}$  and with  $i_W$  becomes regular again. There is little difference in the value of the incremental lift coefficient at corresponding positions above and below the fuselage center line. It may be seen from the figure that increasing wing incidence will increase the incremental lift coefficient at these wing positions.

Figure 4 shows a slight increase in the value of  $\Delta C_{L_W}$  at the higher model lift coefficients as the wing is moved longitudinally toward the rear of the fuselage. At the most rearward position tested, a small decrease in the value of the coefficient was noted. At wing positions above the fuselage,  $\Delta C_{L_W}$  is seen to decrease as the wing moves rearward.

A corresponding increase in the incremental lift coefficient was noticed as the wing moved rearward below the fuselage.

The substitution of a tapered wing with NACA 0018-09 sections into the combination of figure 4 caused a decrease in the incremental lift coefficient with the wing above the fuselage and an increase with the wing below the fuselage. (See fig. 5.) At wing positions on the fuselage, a decrease in  $\Delta C_{LW}$  was noted with the wing at and below the center line, an increase occurring with the wing above the center line. Results at the tangential position again showed large changes taking place. (See fig. 6.)

The addition of fillets to this model (fig. 6) caused noticeable increases in  $\Delta C_{LW}$  with the wing at and above the fuselage center line; decreases in  $\Delta C_{LW}$  were observed at wing positions below the fuselage center line.

A rectangular wing with NACA 4412 section caused a decrease in  $\Delta C_{LW}$  from the values observed in figure 4 with the wing at the fuselage center line. (See fig. 7.) At wing positions off the fuselage, an increase was noted.

The addition of a rectangular fuselage to the combination of figure 4 results in a decrease in the incremental lift coefficient at wing positions on the fuselage and above the center line and an increase when the wing is below the fuselage center line. (See fig. 8.) An increase in  $\Delta C_{LW}$  was noted at both tangential positions, and at wing positions off the fuselage an increase resulted above and a decrease below.

The addition of fillets to the model of figure 8 caused a decrease in  $\Delta C_{LW}$  with the wing at the fuselage center line and an increase at a wing position on the fuselage and below the center line. The change in the incremental lift coefficient at the wing position on the fuselage and above the center line was insignificant.

Substituting wings with NACA 0018-09 and NACA 4412 sections into the combination of figure 8 (figs. 9 and 10) caused trends similar to those previously observed in figures 5, 6, and 7.

The results presented in figures 4 to 10 indicate that the incremental lift coefficient is affected to a greater extent by position changes of the wing with respect to the fuselage than by modifications to the model. The vertical position at which the wing was tangent to the fuselage caused the greatest change in the incremental lift coefficient. Lesser variations were caused by wing incidence. The incremental lift coefficient is affected to the next greatest extent by the presence of fillets. Increased wing camber (NACA 4412 airfoil) will result in a lesser change in  $\Delta C_{LW}$  while varying fuselage shape and the introduction of wing

taper and increased root thickness (NACA 0018-09 airfoil) account for still smaller variations. The effects of varying the horizontal position of the wing on the fuselage are negligible.

The accuracy of the data of figures 4 to 10 is the same as that of the usual airfoil tests. (See reference 9.) In general, the error in the measured lift coefficient is not greater than  $\pm 0.02$ .

### Wing-Nacelle Interference

Figure 12 shows that at  $0^\circ$  angle of attack the nacelle in the midposition ( $Z = 0$ ) has a slight positive lift. Lowering the nacelle reduces the lift increment. The nacelle in the high position ( $Z = 0.18$ ) contributes some lift, which, unlike that measured for the other positions, increases with Mach number. At the higher angles of attack the lift increments become more positive with increasing Mach number.

The results of the tests of the horizontal variation of nacelle position (fig. 13) show that moving the nacelle forward on the wing increases the loss in lift due to the nacelle. The lift increments decrease with increasing Mach number for the more forward positions of the nacelle at an angle of attack of  $0^\circ$ , and for rearward nacelle positions as the angle of attack increases.

The results from the angular variation tests, shown in figure 14, indicate the lift to be greatest for the nacelle having a positive angle of incidence. The lift increments become more positive with increasing Mach number at the higher angle of attack.

Figures 12 to 14 indicate trends similar to those previously noted for wing-fuselage combinations. The variations in  $\Delta C_{L_N}$  due to increasing Mach number are so small as to be negligible within the range of the tests. The effect of the angle of attack upon the incremental lift coefficient appears to be insignificant for the attitudes tested.

The test points from which these curves were plotted indicate maximum discrepancies in  $\Delta C_{L_N}$  between 0.002 and -0.004.

Although the results presented in figures 3 to 14 seem to contradict the consistency of these data of figures 1 and 2 and table I, these may be due to the breakup of the interference lift between components. No definite conclusions can be drawn from this data unless tests of the datum configuration in which loads are measured on the wings in the presence of the fuselage were available.

## CONCLUSIONS

An analysis of the available data on the effects of wing-fuselage-tail and wing-nacelle interference on the distribution of the air load among components of airplanes has led to the following conclusions:

1. There is little apparent variation of the division of the air load between the components of the airplane with Mach number within the range of the available flight tests. As a result, the present assumption that fuselage lift may be considered as the lift acting on the portion of wing area blanketed by the body is valid over the subsonic Mach number range in the cases of the two airplanes.

2. The incremental lift coefficient due to the interference varies regularly with model lift coefficient and wing incidence except at vertical wing positions near the tangential. Here large changes in the incremental lift coefficient become evident.

3. Other variables such as horizontal wing movement, angle of incidence, filleting, fuselage shape, and airfoil section influence the incremental lift coefficient to lesser degrees.

4. Nacelle incidence and position affect the incremental lift coefficient as in wing-fuselage combinations. The effect of Mach number upon the coefficient is negligible within the range of the tests.

5. Although indirect data have been analyzed to obtain trends, they are not applicable to determine the division of the air load among the components of airplanes. Further direct experimental data are necessary before indirect data may be used to determine the division of load.

Langley Aeronautical Laboratory  
National Advisory Committee for Aeronautics  
Langley Air Force Base, Va.

## REFERENCES

1. Beeler, De E., and Mayer, John P.: Measurements of the Wing and Tail Loads during the Acceptance Tests of Bell XS-1 Research Airplane. NACA RM No. L7L12, 1948.
2. Aiken, William S., Jr.: Flight Determination of Wing and Tail Loads on a Fighter-Type Airplane by Means of Strain-Gage Measurements. NACA TN No. 1729, 1948.
3. Jacobs, Eastman N., and Ward, Kenneth E.: Interference of Wing and Fuselage from Tests of 209 Combinations in the N.A.C.A. Variable-Density Tunnel. NACA Rep. No. 540, 1935.
4. Sherman, Albert: Interference of Wing and Fuselage from Tests of 28 Combinations in the N.A.C.A. Variable-Density Tunnel. NACA Rep. No. 575, 1936.
5. Lennertz, J.: On the Mutual Reaction of Wings and Body. NACA TM No. 400, 1927.
6. Multhopp, H.: Aerodynamics of the Fuselage. NACA TM No. 1036, 1942.
7. Spreiter, John R.: Aerodynamic Properties of Slender Wing-Body Combinations at Subsonic, Transonic, and Supersonic Speeds. NACA TN No. 1662, 1948.
8. McLellan, Charles H., and Cangelosi, John I.: Effects of Nacelle Position on Wing-Nacelle Interference. NACA TN No. 1593, 1948.
9. Jacobs, Eastman N., Ward, Kenneth E., and Pinkerton, Robert M.: The Characteristics of 78 Related Airfoil Sections from Tests in the Variable-Density Wind Tunnel. NACA Rep. No. 460, 1933.

TABLE I  
COMPARISON OF EXPERIMENTAL LIFT-SLOPES OF COMPONENTS  
OF TEST AIRPLANES WITH VALUES OBTAINED  
UNDER ASSUMPTION

X-1

	Experiment	Calculation	
		Strip	Lifting line
$dC_{LW}/dC_{LA}$	0.78	0.765	0.758
$dC_{LF}/dC_{LA}$	.23	.235	.242

TEST AIRPLANE OF REFERENCE 2

	Experiment	Calculation	
		Strip	Lifting line
$dC_{LW}/dC_{LA}$	0.78	0.808	0.797
$dC_{LF}/dC_{LA}$	.21	.192	.203



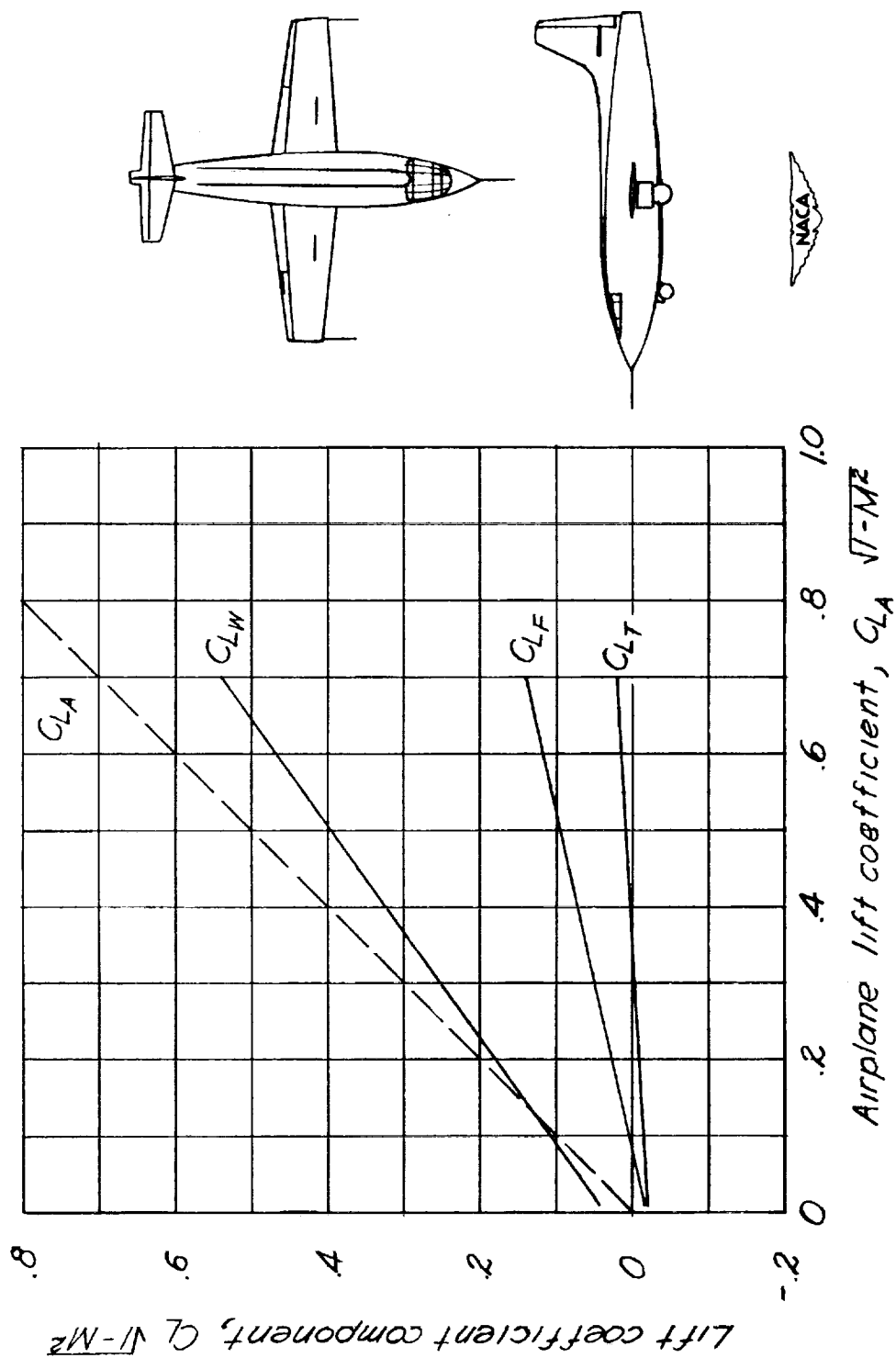


Figure 1. - Components of lift coefficient due to wing, fuselage and tail; X-1 airplane;  $0.27 < M < 0.80$  (from reference 1).

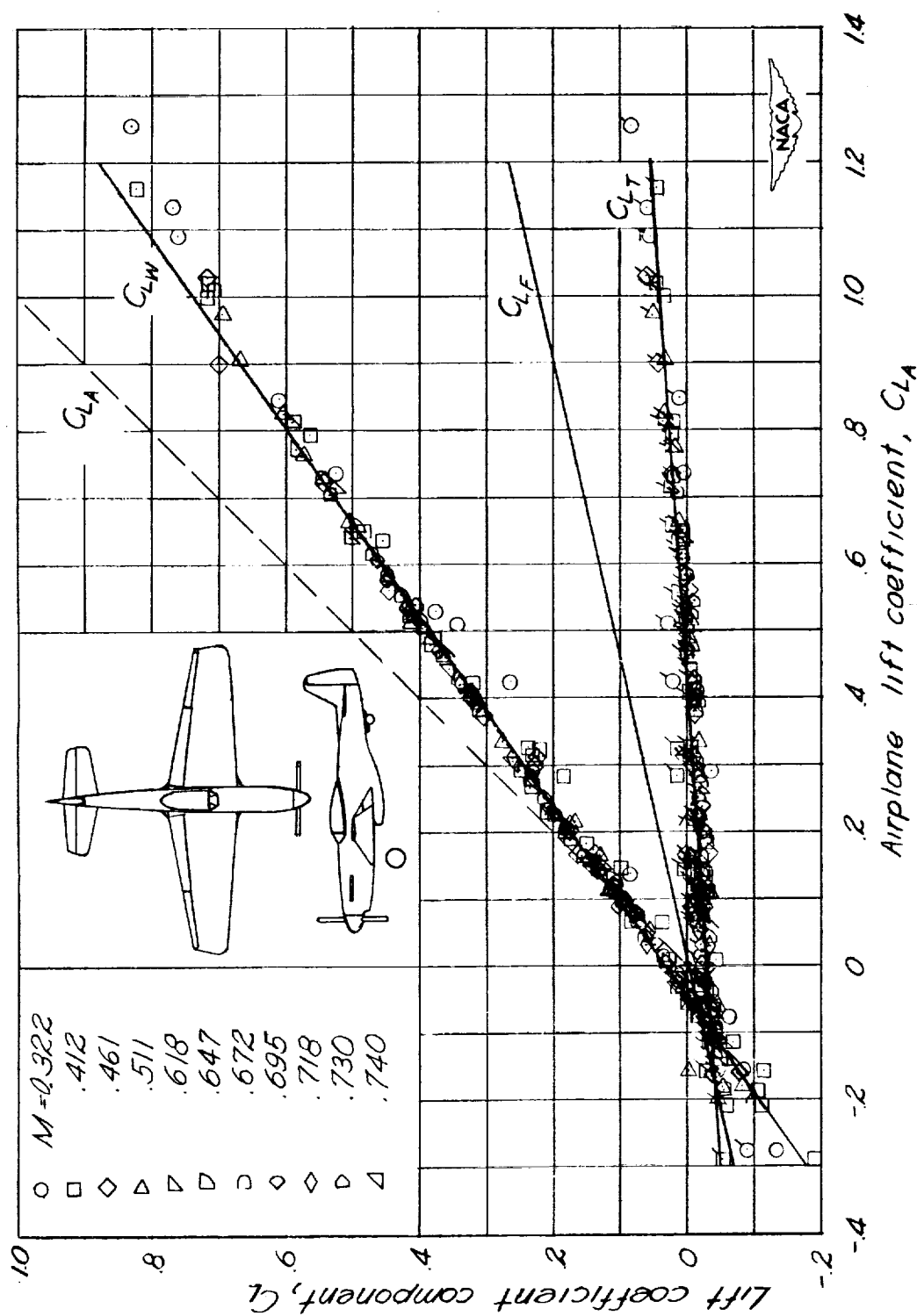


Figure 2. - Components of lift coefficient due to wing, fuselage, and tail; test airplane of reference 2.

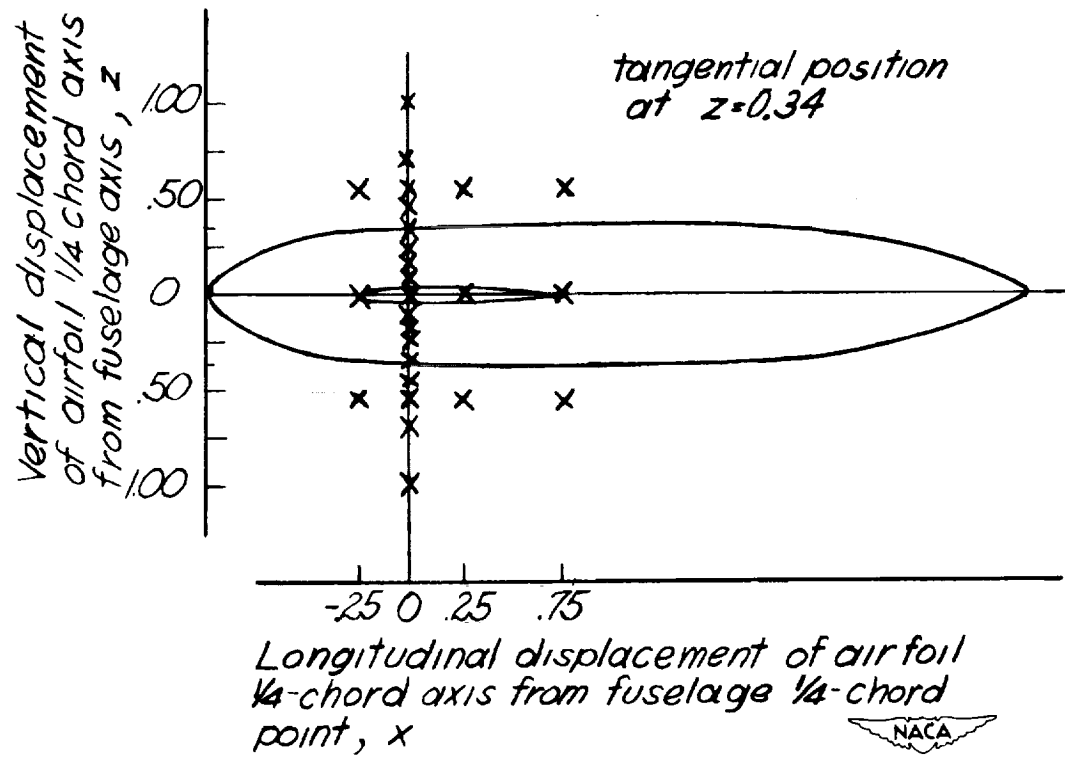


Figure 3 :- Diagram of various wing positions, with respect to fuselage, considered in figures 4 to 10.

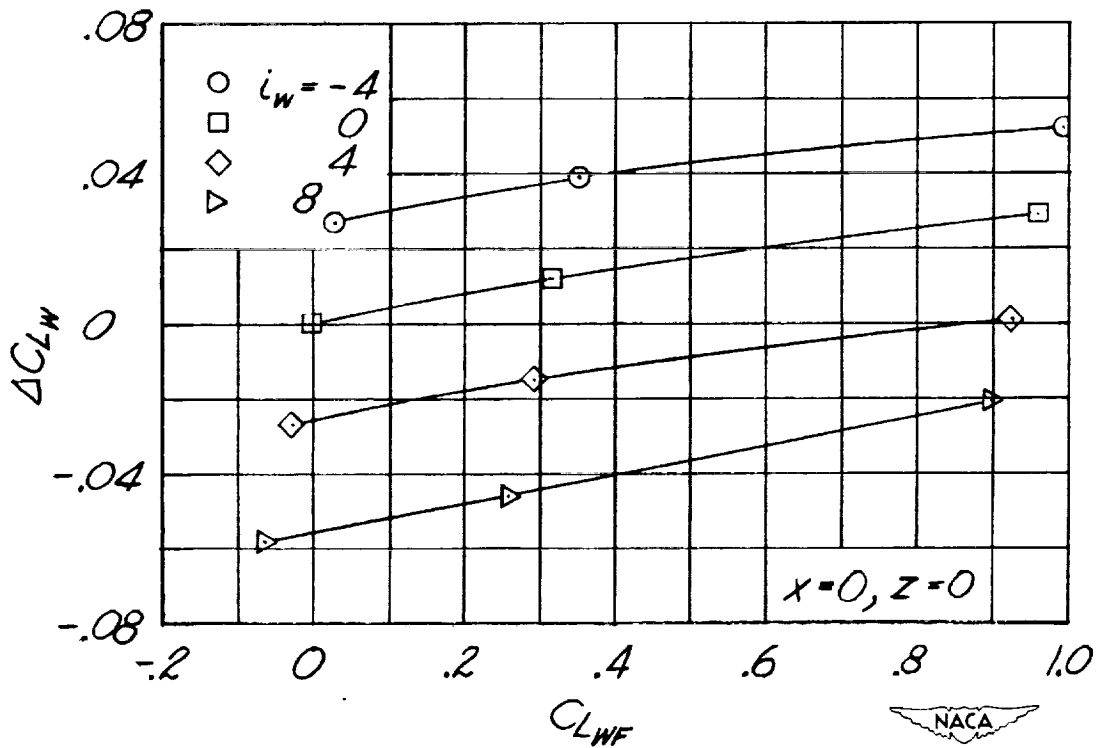


Figure 4.- Variation of incremental wing lift coefficient with model lift coefficient. Rectangular wing with NACA 0012 section and round fuselage.

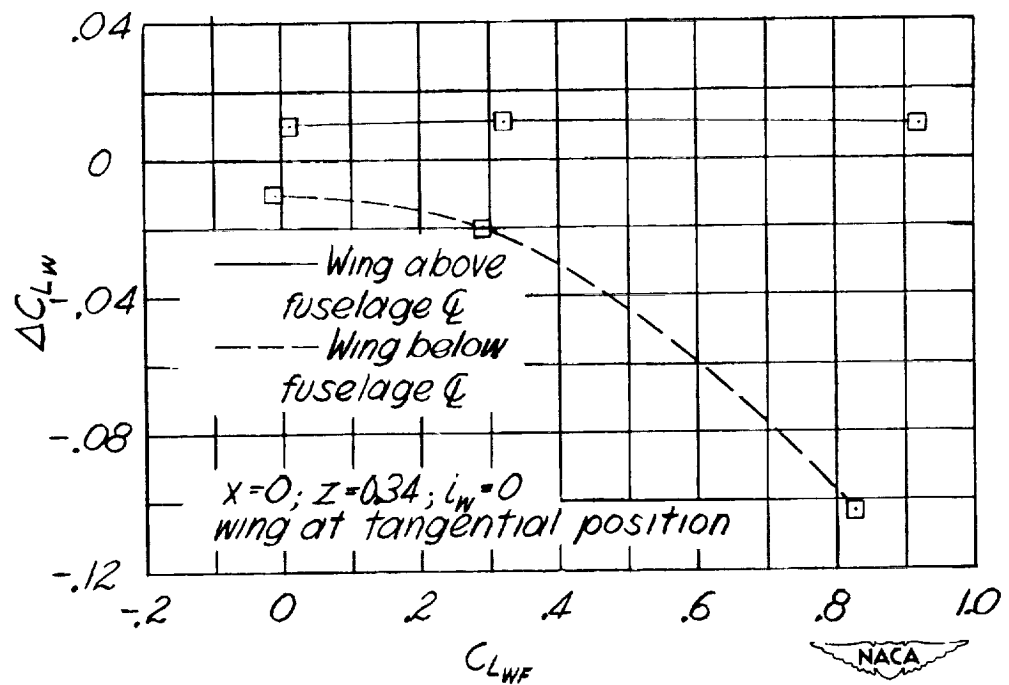
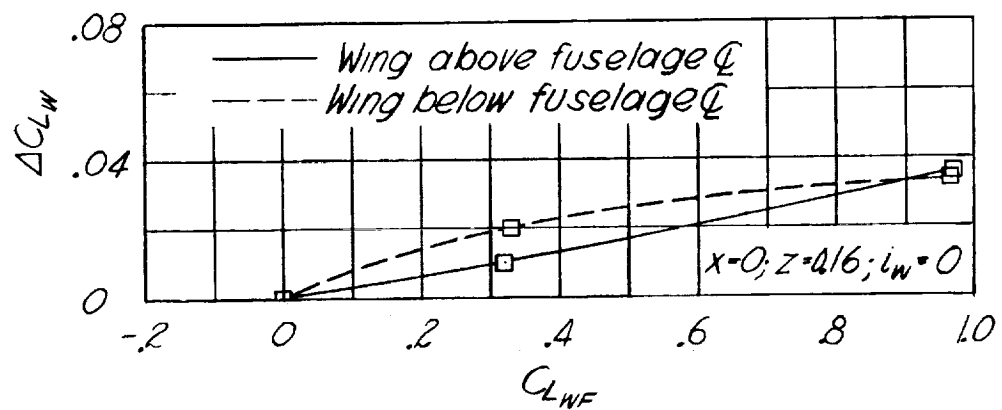
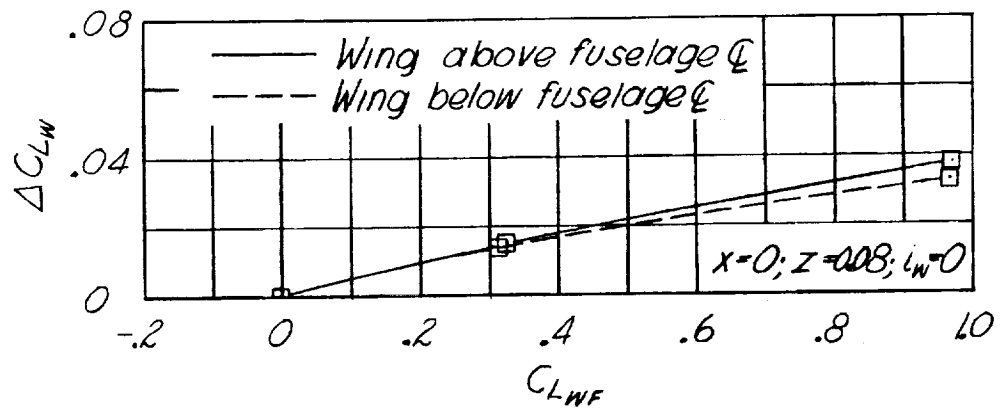


Figure 4 . - Continued.

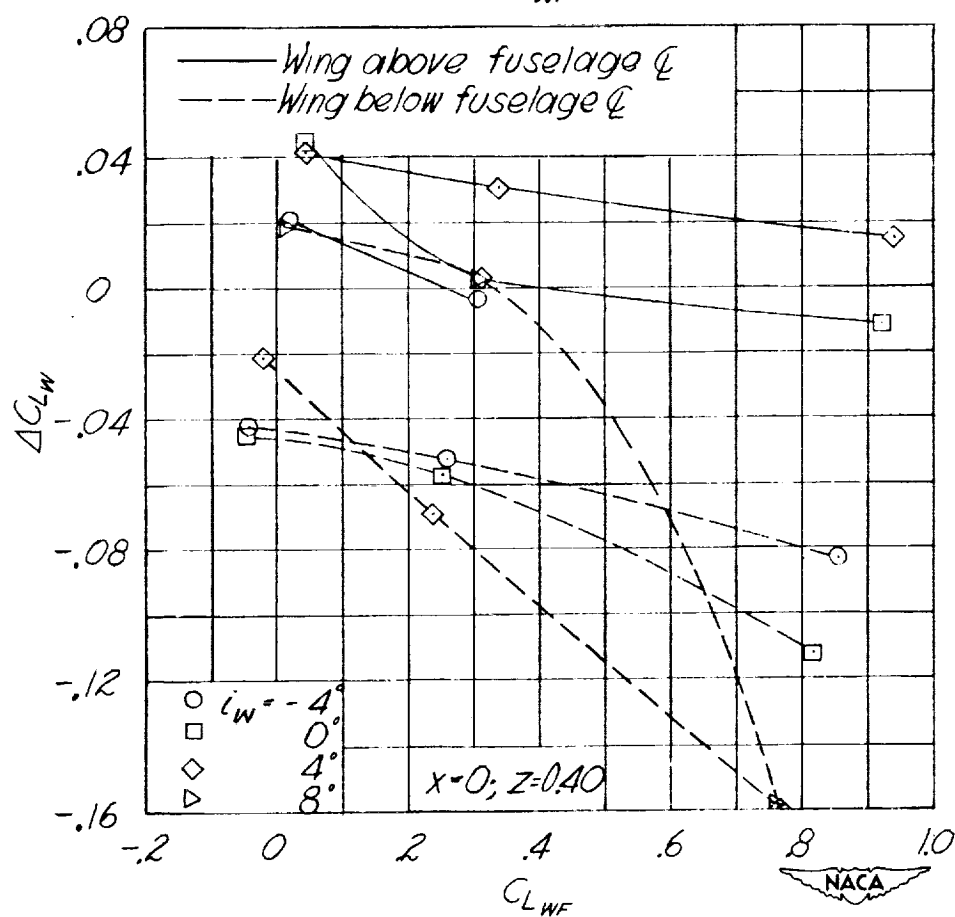
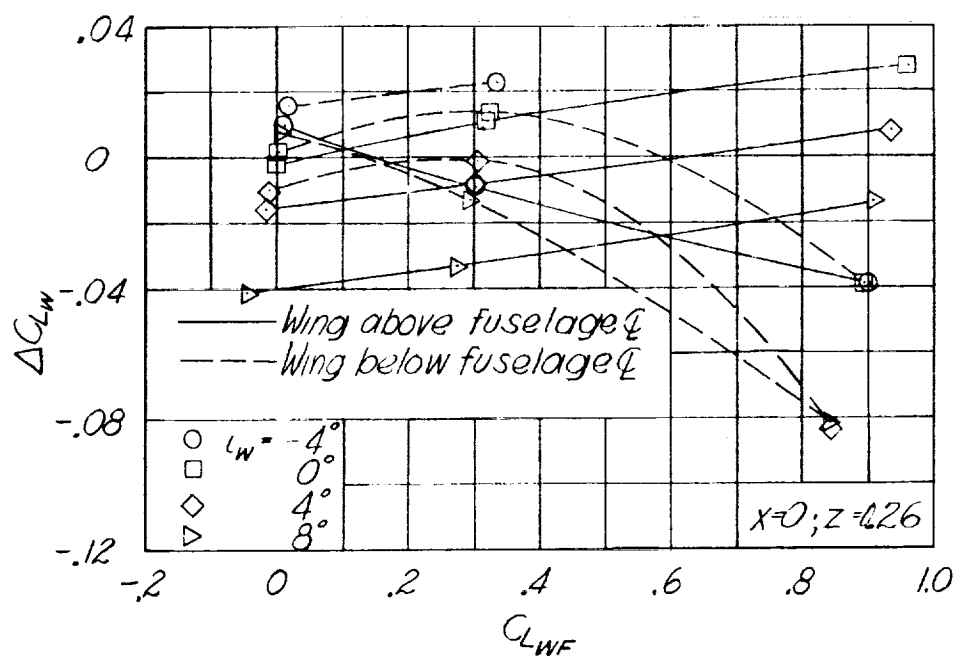


Figure 4. - Continued.

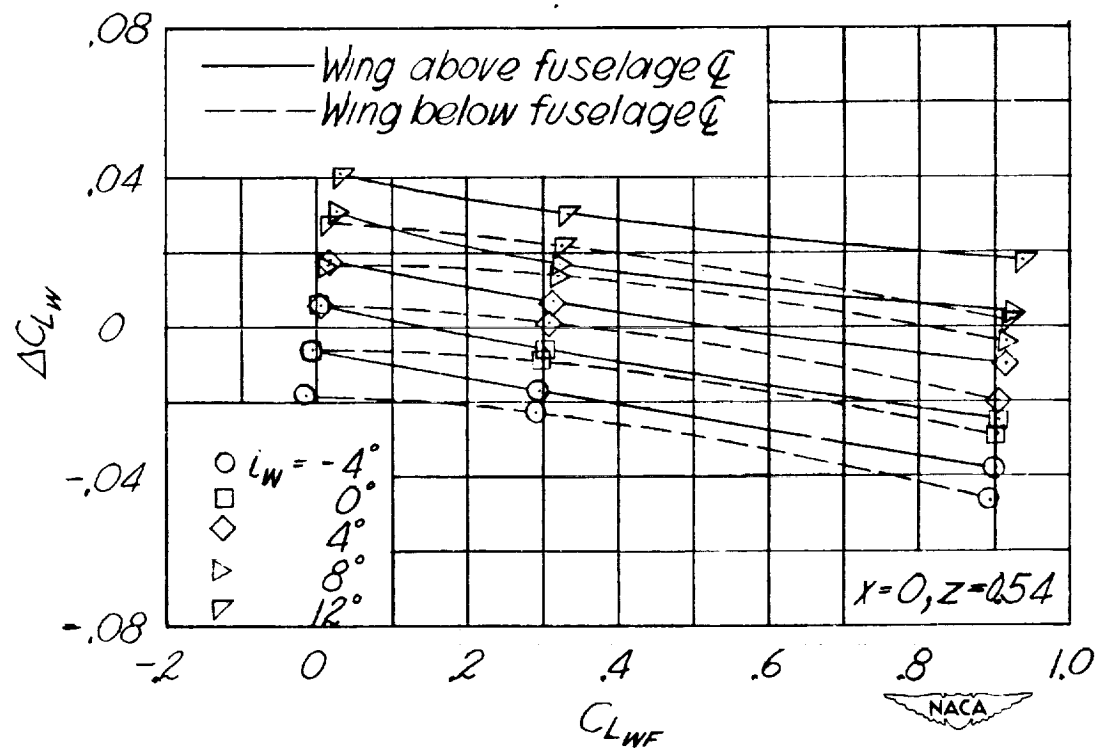
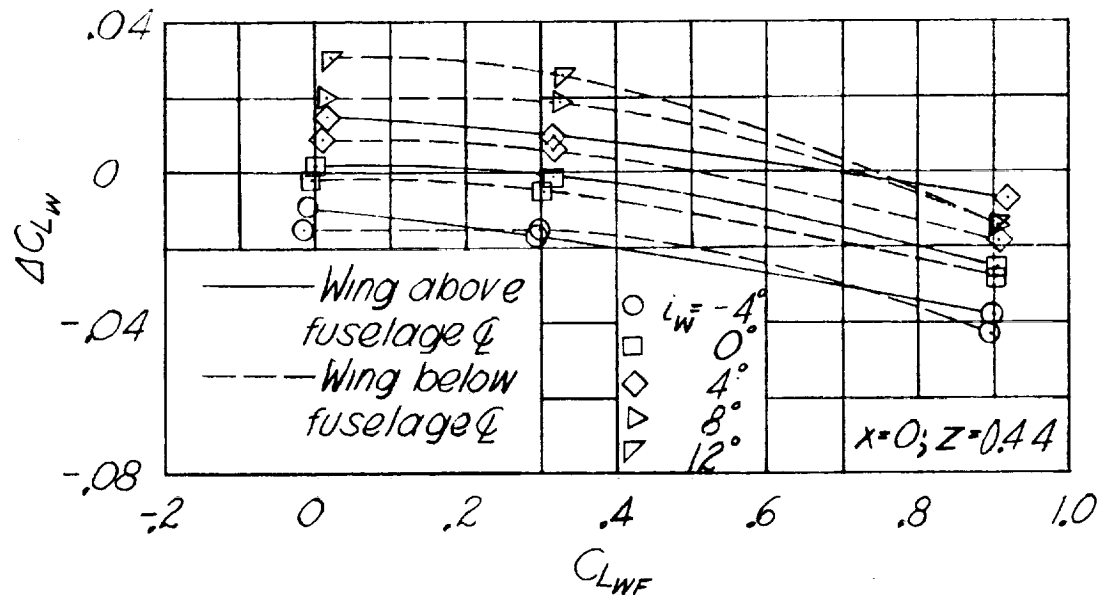


Figure 4. - Continued.

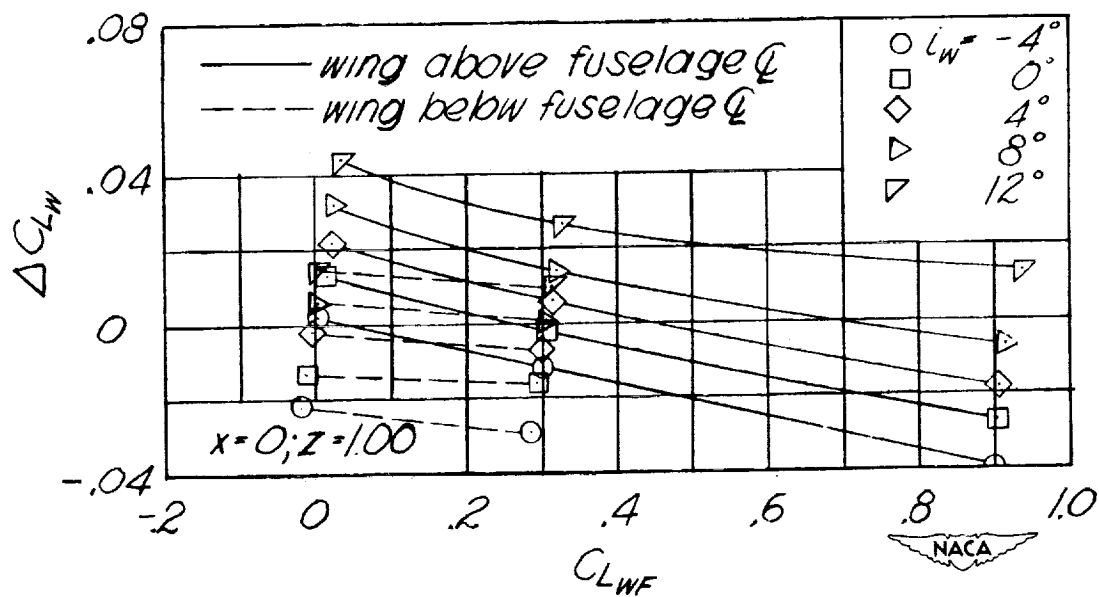
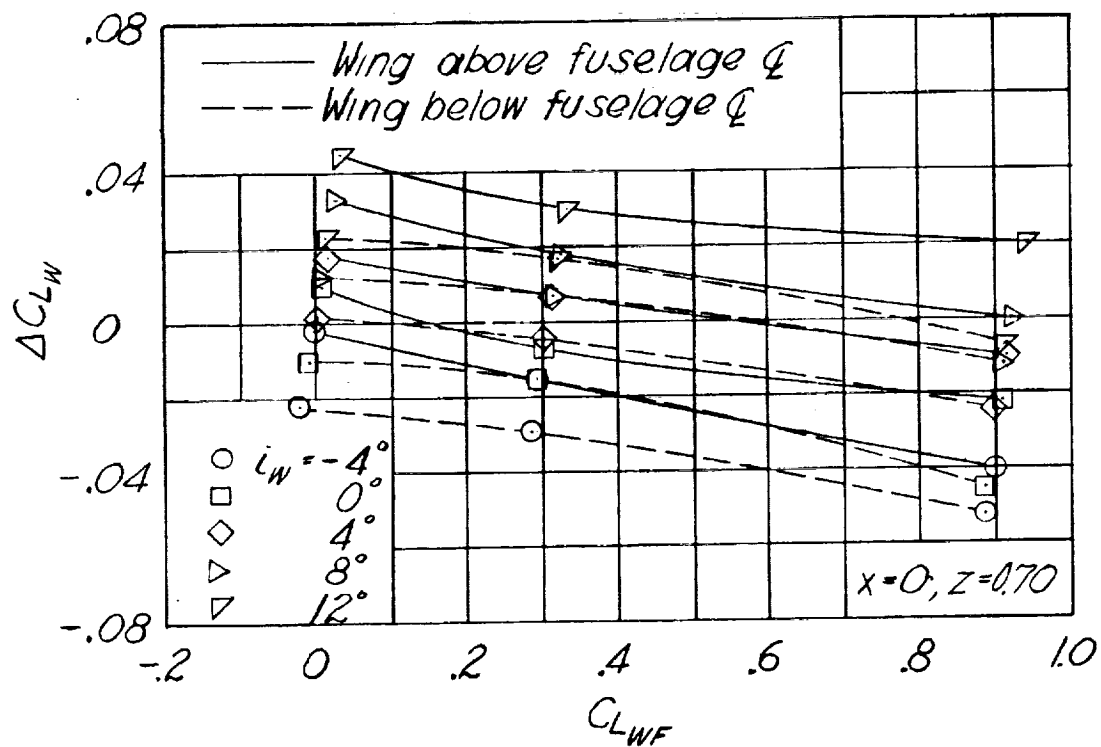


Figure 4.- Continued.

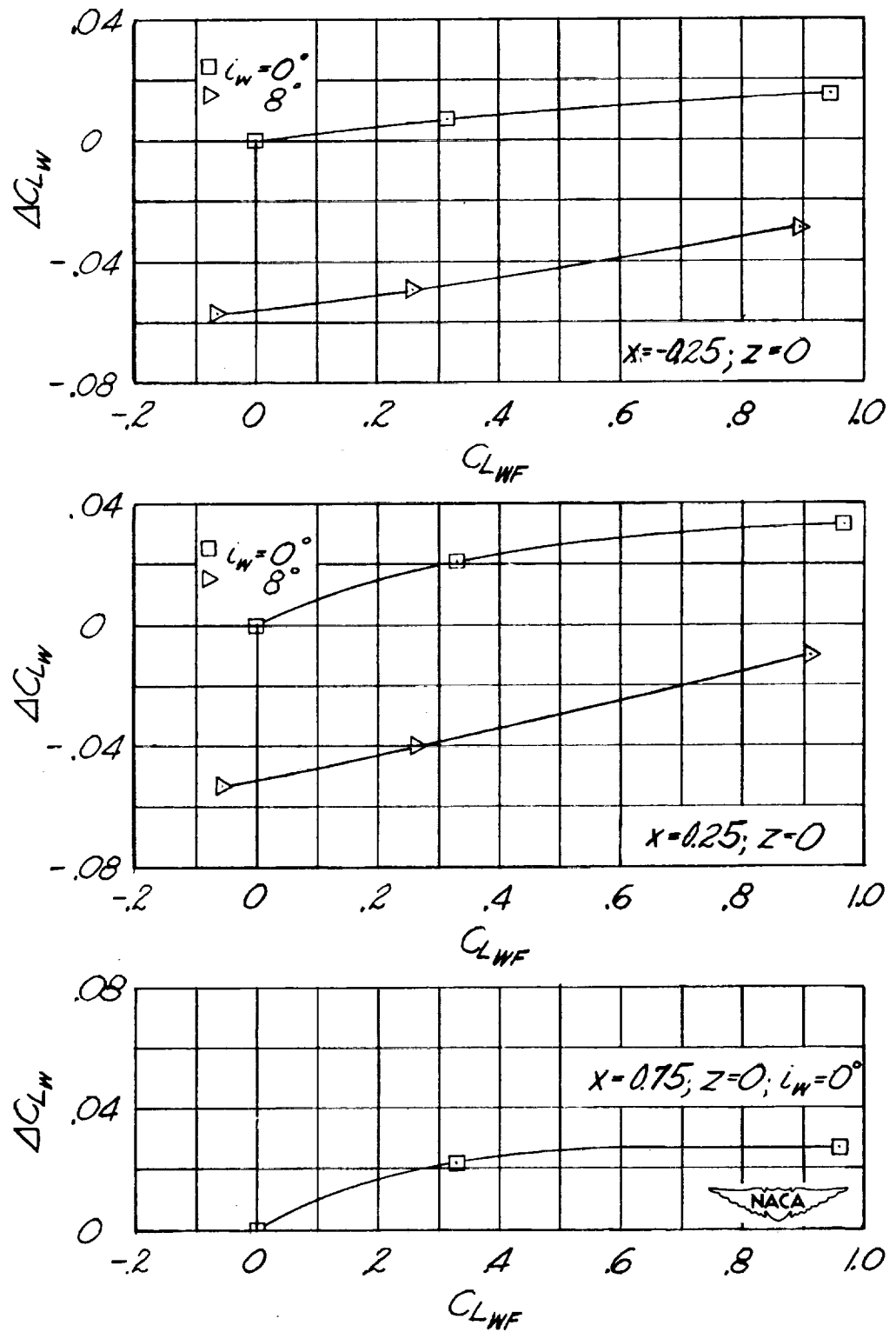


Figure 4 - Continued.

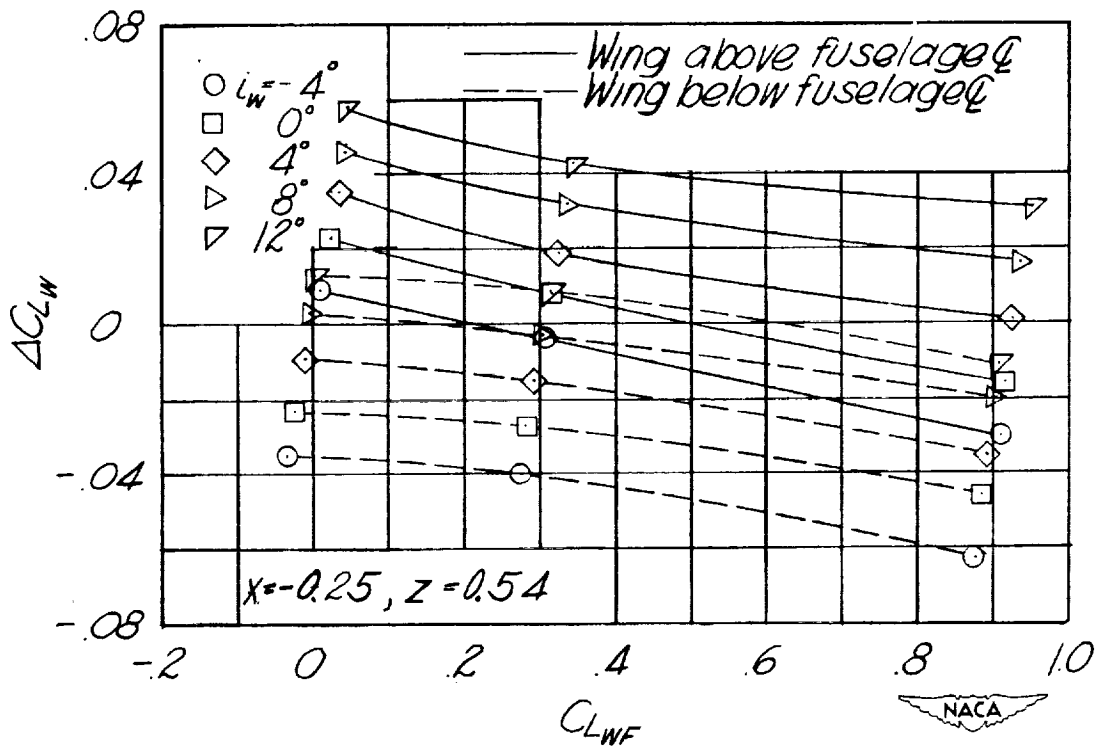


Figure 4.- Continued.

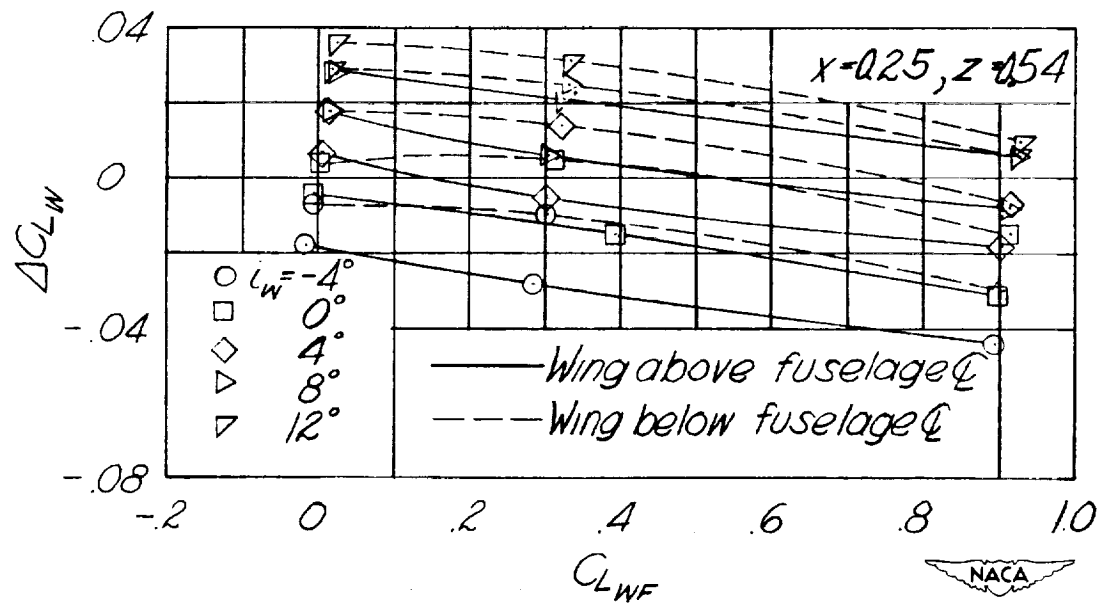


Figure 4.- Continued.

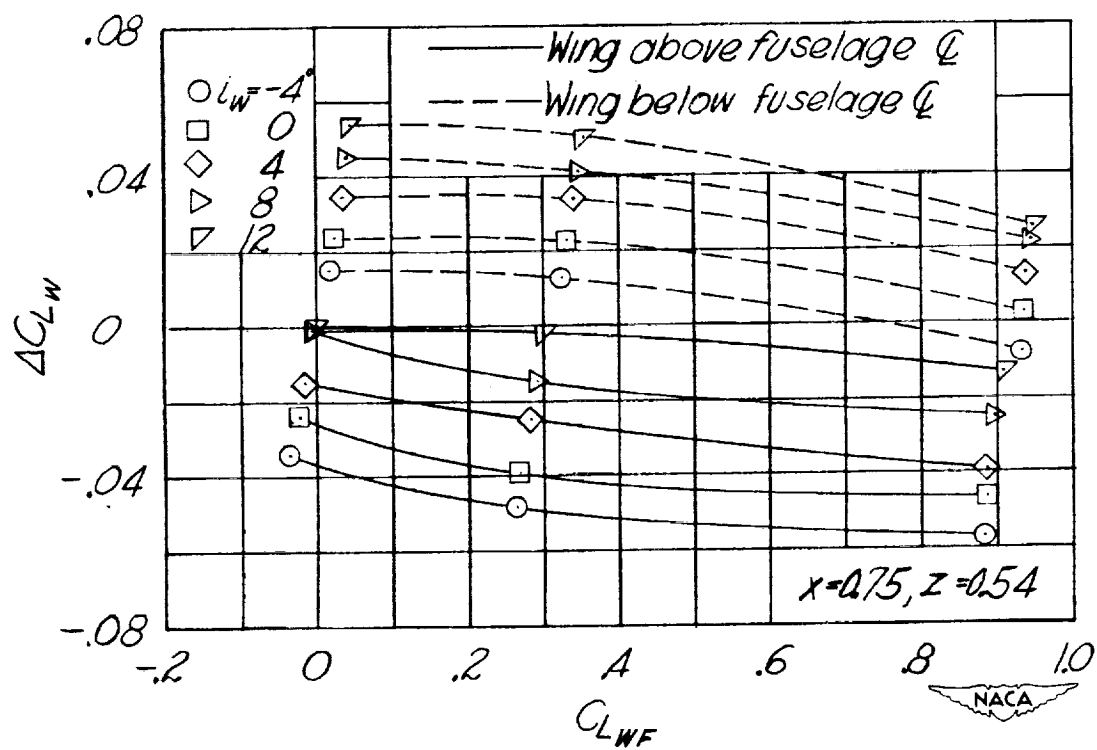


Figure 4.- Concluded.

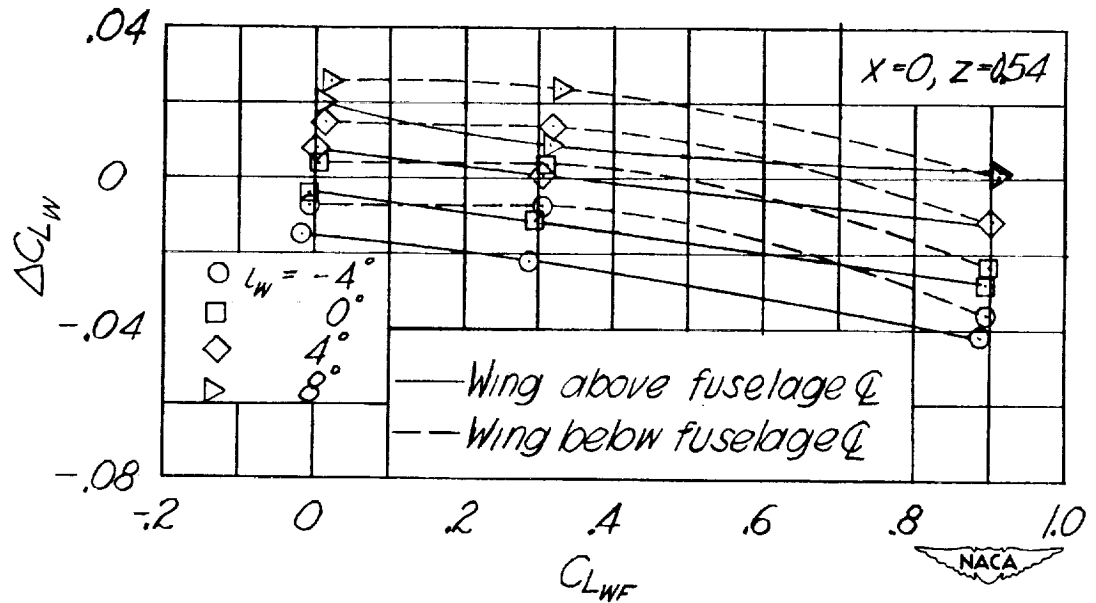
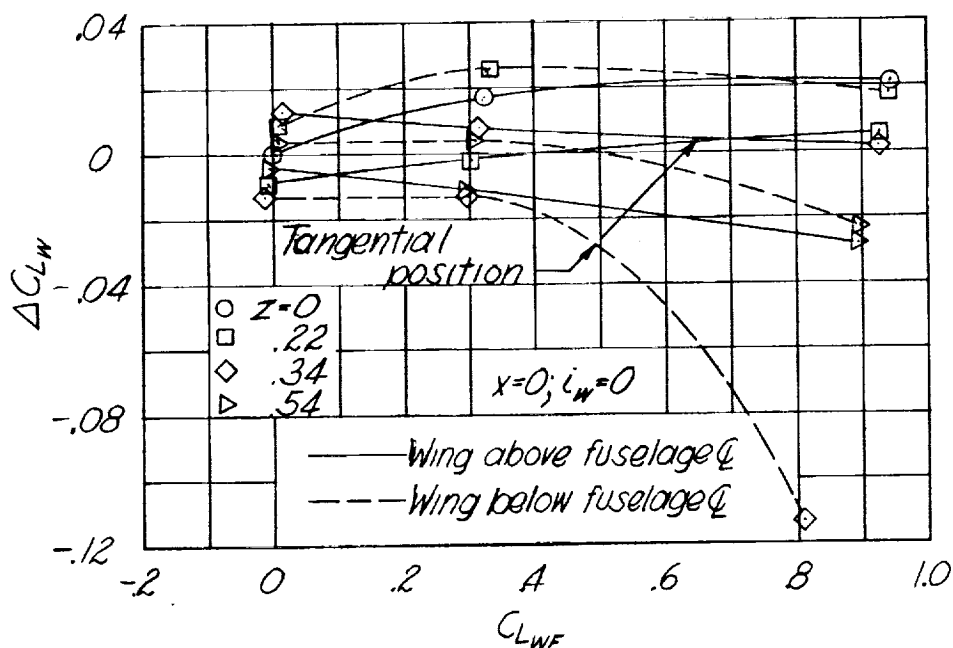
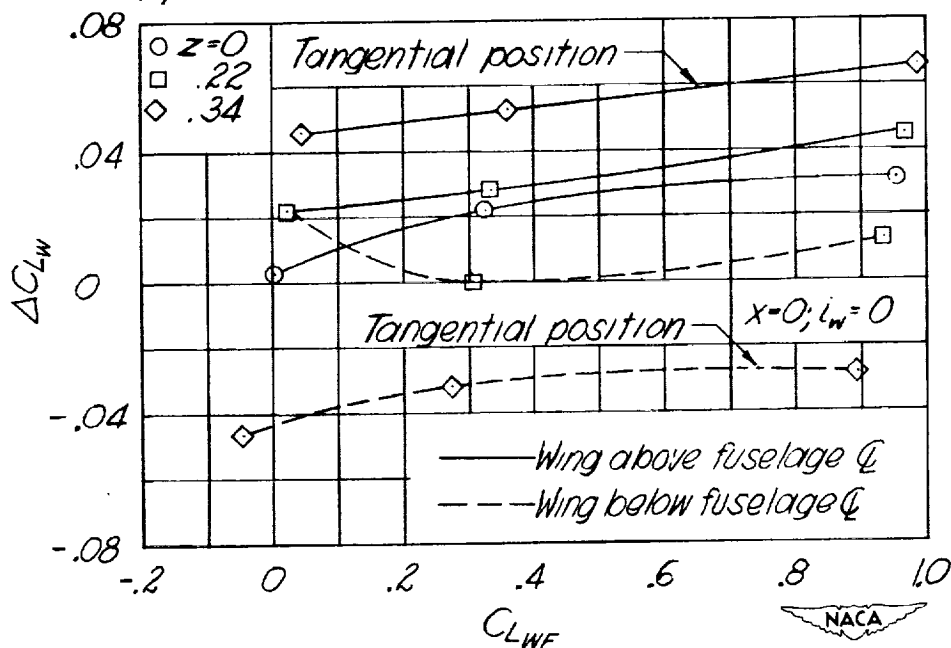


Figure 5.- Variation of incremental wing lift coefficient with model lift coefficient. Tapered wing with NACA 0018-09 sections and round fuselage.



(a) - Model without fillets.



(b) - Model with tapered fillets.

Figure 6. - Variation of incremental wing lift coefficient with model lift coefficient. Tapered wing with NACA 0018-09 sections and round fuselage.

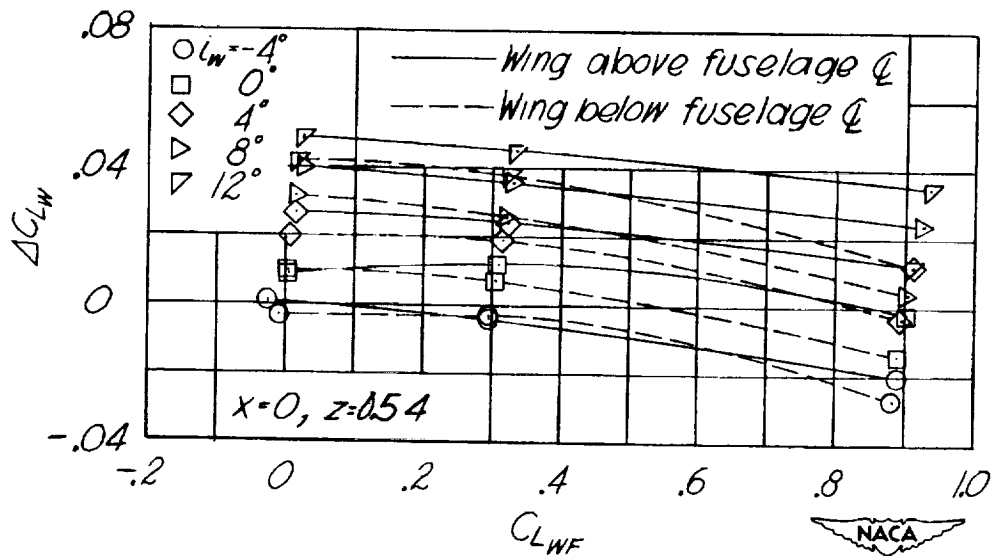
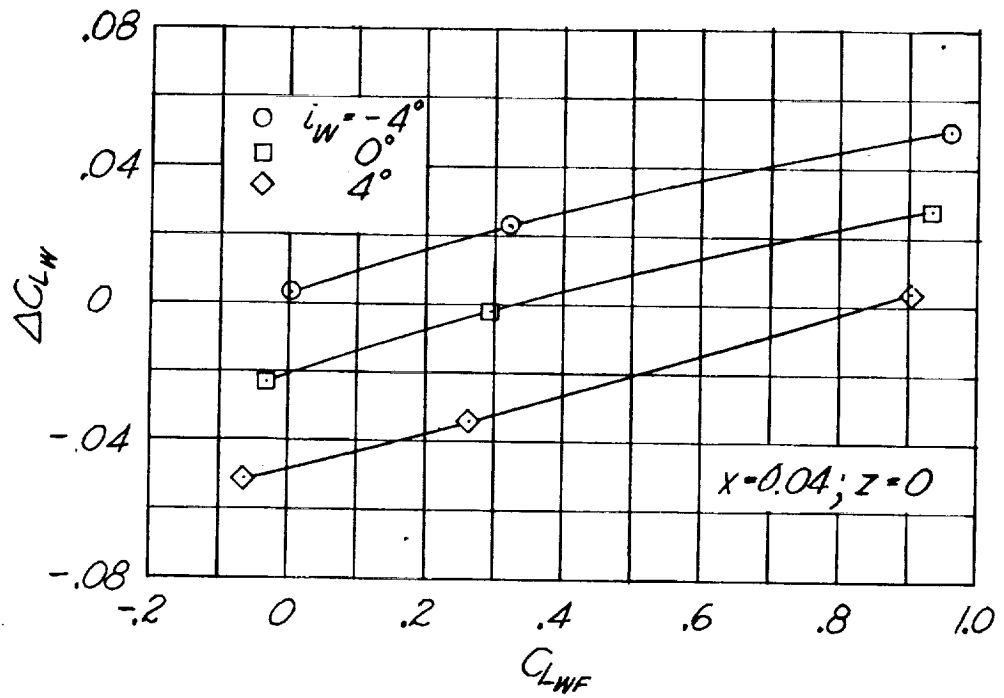
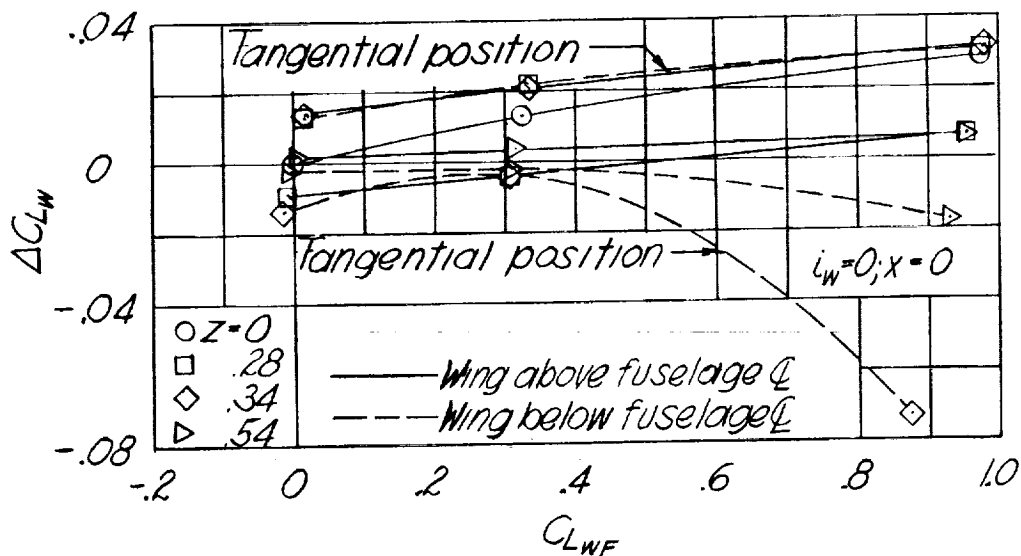
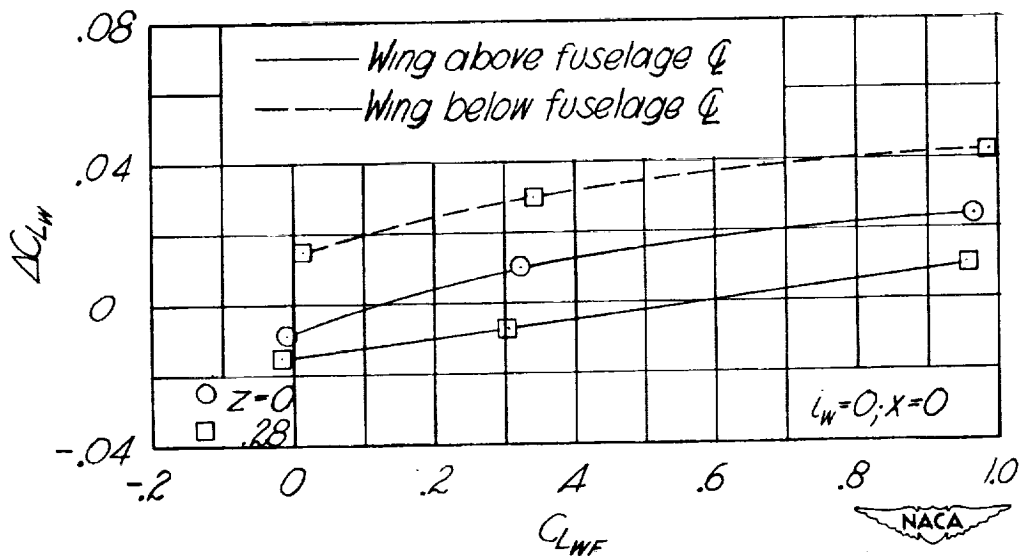


Figure 7.- Variation of incremental wing lift coefficient with model lift coefficient. Rectangular wing with NACA 4412 section and round fuselage.



(a) - Model without fillets.



(b) - Model with tapered fillets.

Figure 8.- Variation of incremental wing lift coefficient with model lift coefficient. Rectangular wing with NACA 0012 section and rectangular fuselage.

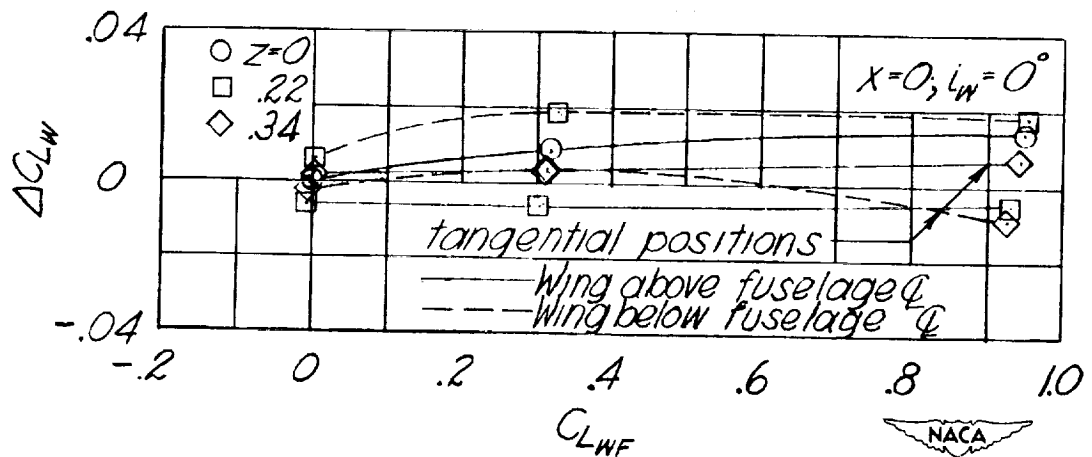


Figure 9.- Variation of incremental wing lift coefficient with model lift coefficient. Tapered wing with NACA 0018-09 sections and rectangular fuselage.

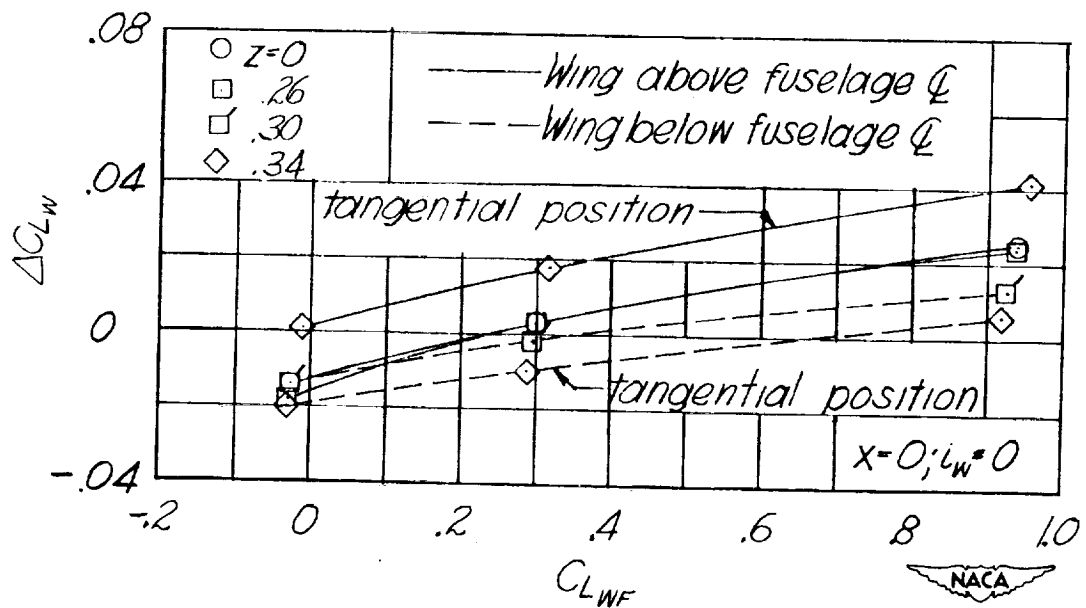


Figure 10.- Variation of incremental wing lift coefficient with model lift coefficient. Rectangular wing with NACA 4412 section and rectangular fuselage.

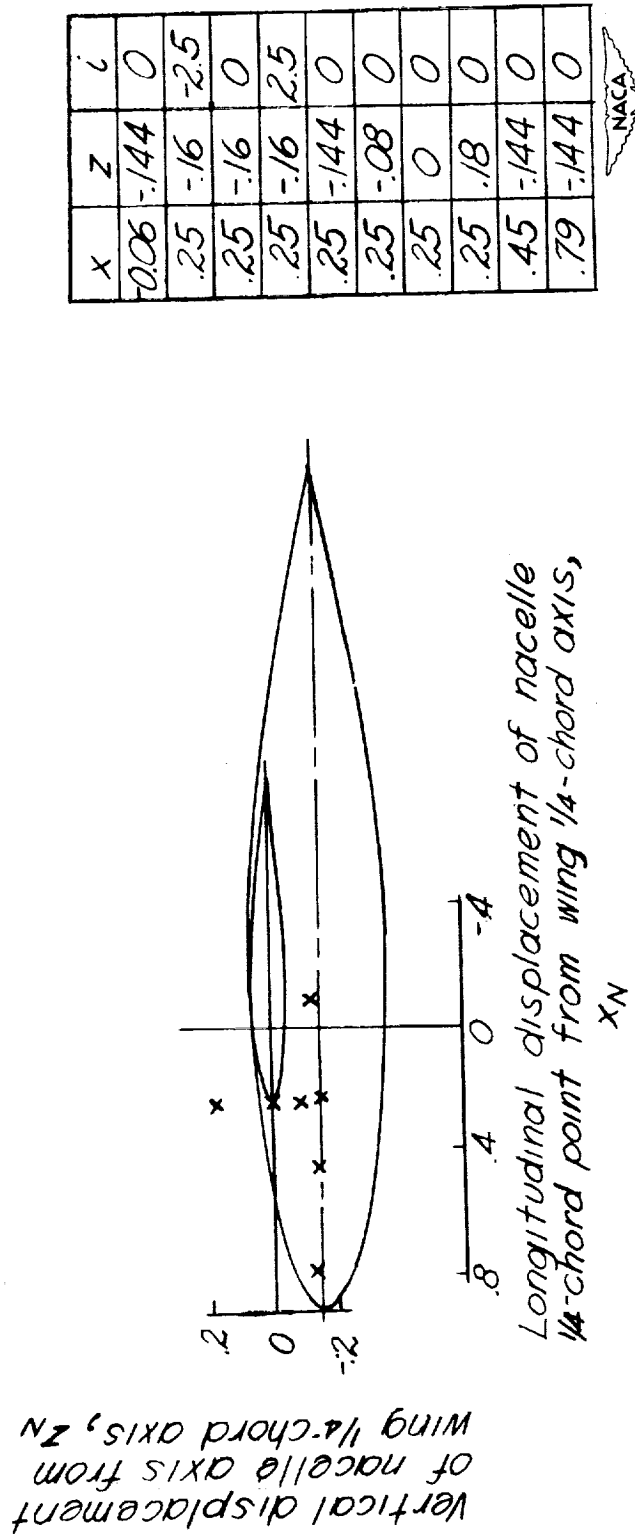


Figure 11.- Diagram of various nacelle positions, with respect to wing, considered in figures 12 to 14.

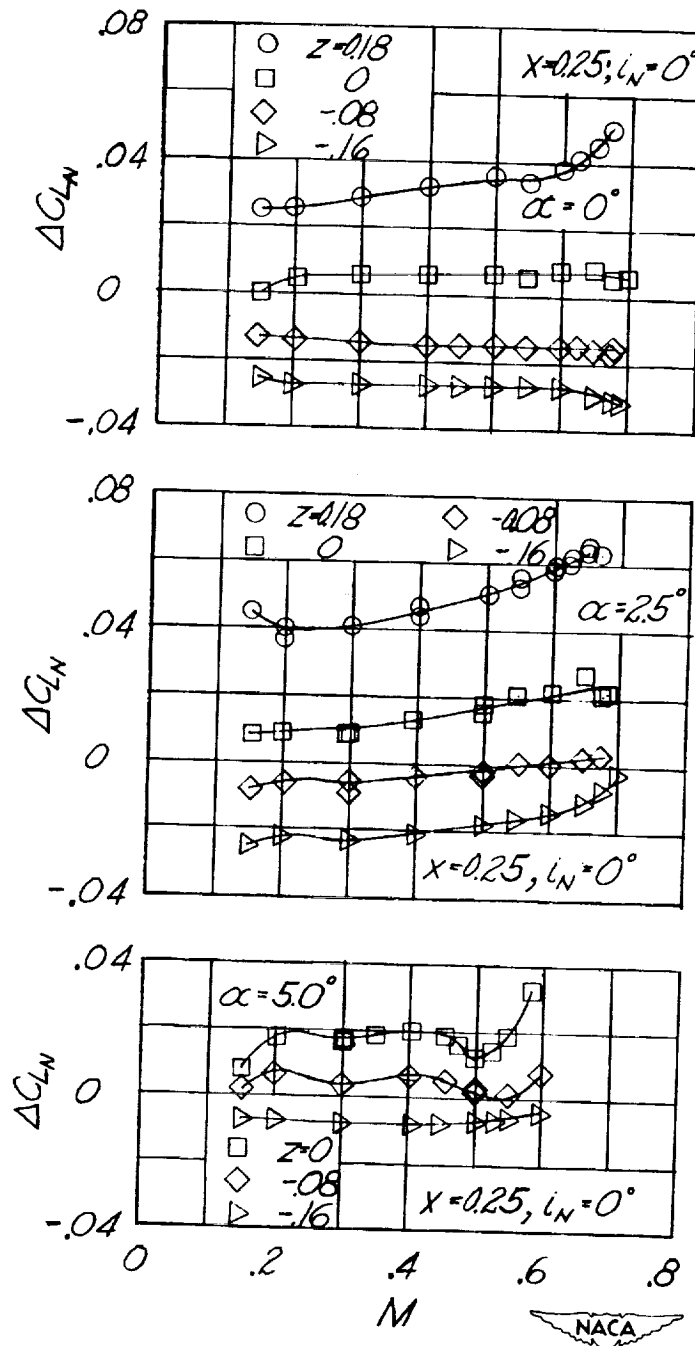


Figure 12 - Variation of incremental nacelle lift coefficient with Mach number. Modified NACA fuselage form III with fineness ratio 6.0 and modified NACA 65-210 airfoil.

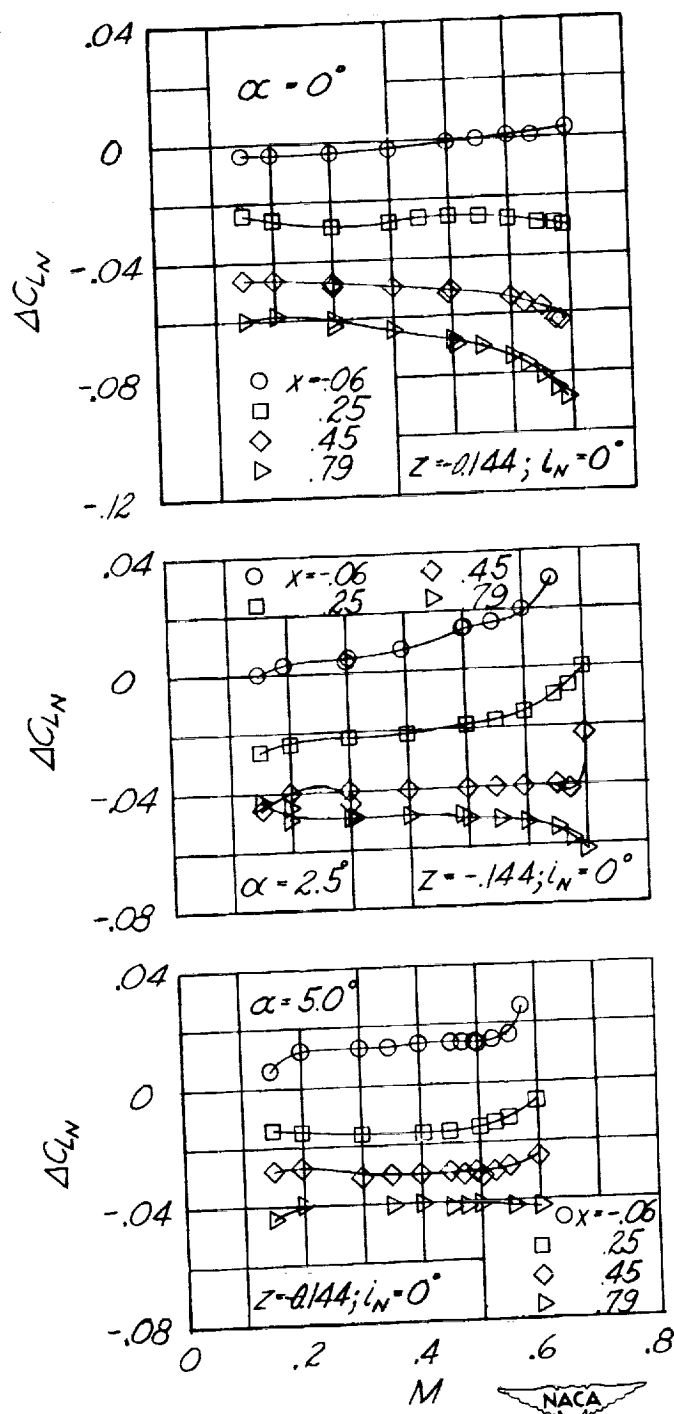


Figure 13 - Variation of incremental nacelle lift coefficient with Mach number. Modified NACA fuselage form III with fineness ratio 6.0 and modified NACA 65-210 airfoil.

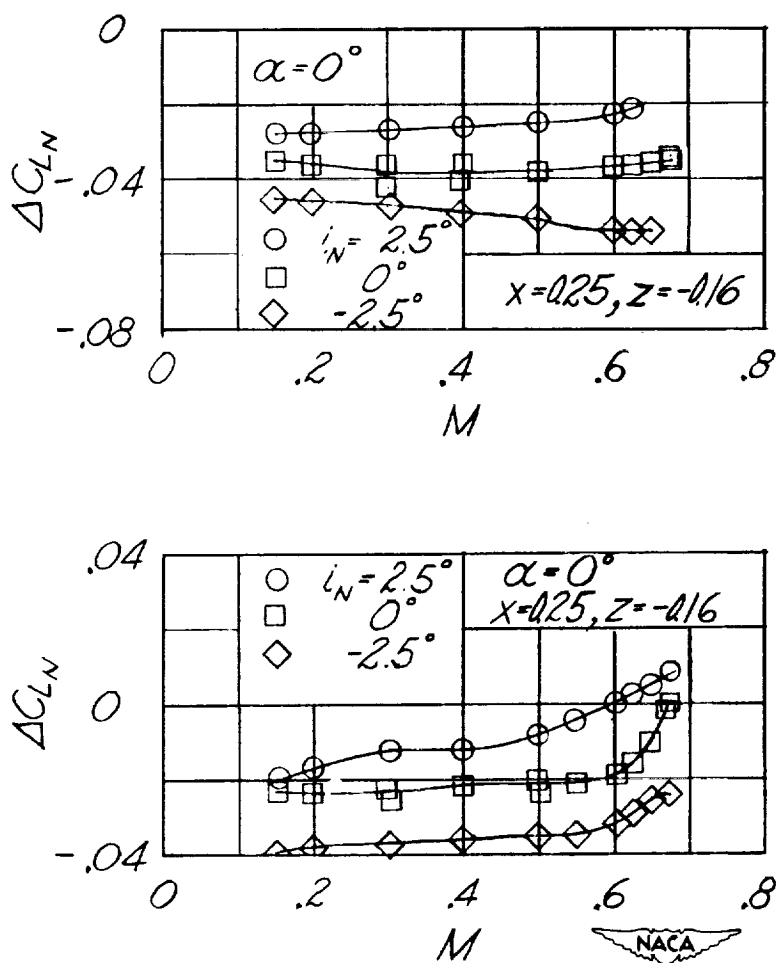


Figure 14.- Variation of incremental nacelle lift coefficient with Mach number. Modified NACA fuselage form III with fineness ratio 6.0 and modified NACA 65-210 airfoil.

